12-2006

Near-Field Thermal Radiative Transfer and Thermoacoustic Effects from Vapor Plumes Produced by Pulsed CO/sub 2 /Laser Ablation of Bulk Water

S. I. Kudryashov
Arkansas State University

Kevin Lyon
Arkansas State University

S. D. Allen
Arkansas State University - Main Campus, allens17@erau.edu

Scholarly Commons Citation

Kudryashov, S. I., Lyon, K., & Allen, S. D. (2006). Near-Field Thermal Radiative Transfer and Thermoacoustic Effects from Vapor Plumes Produced by Pulsed CO/sub 2 /Laser Ablation of Bulk Water. *Journal of Applied Physics, 100*(12). https://doi.org/10.1063/1.2402388

Near-field thermal radiative transfer and thermoacoustic effects from vapor plumes produced by pulsed CO_2 laser ablation of bulk water

S. I. Kudryashov,[a] Kevin Lyon, and S. D. Allen
Department of Chemistry and Physics, Arkansas State University, Jonesboro, Arkansas 72467-0419

(Received 6 May 2006; accepted 11 October 2006; published online 26 December 2006)

Submillimeter deep heating of bulk water by thermal radiation from ablative water plumes produced by a 10.6 μm transversely excited atmospheric CO_2 laser and the related acoustic generation has been studied using a contact time-resolved photoacoustic technique. Effective penetration depths of thermal radiation in water were measured as a function of incident laser fluence and the corresponding plume temperatures were estimated. The near-field thermal and thermoacoustic effects of thermal radiation in laser-ablated bulk water and their potential near-field implications are discussed. © *2006 American Institute of Physics*. [DOI: 10.1063/1.2402388]

I. INTRODUCTION

Intense thermal laser ablation of liquids and solids is usually associated with their heating well above corresponding normal boiling temperatures, resulting in hot vapor/droplet plumes or even ablative plasma.[1,2] Such ablative plumes or hot plasmas exhibit significant mechanical and optical effects on laser removal of the ablated target material related, respectively, to recoil pressure of ablated products[1,2] or their screening effect.[1–3] However, the accompanying thermal effects in target materials induced by thermal "blackbody" emission of ablative plumes or plasmas, e.g., ultradeep plasma-assisted drilling of opaque solids,[4] have only been studied in the high-power laser ablation regime,[1,2,4,5] which allows routine optical, x-ray, or mass-spectroscopic studies of laser-generated hot plasmas.[1–3] In contrast, laser nano- and microstructurings of solid and soft matter (e.g., polymer or foam) surfaces[2,6] or surgical ablation of biological tissues[7] is typically associated with low-temperature weakly or nonionized ablative plumes ($kT \sim 0.1$ eV $\ll I_p \sim 10$ eV, where k is the Boltzmann constant and I_p is the first ionization potential of ablated atomic or molecular species). These ablative plumes may significantly affect the results of surface structuring via their blackbody emission, changing the dimensions of the heat-affected zone and initiating near-field thermomechanical or thermoacoustic effects. Unfortunately, experimental studies of the impact of such thermal emission on laser ablation of solids and liquids at moderate temperatures are very complicated due to the opacity of most condensed matter in the corresponding mid- and far-IR spectral ranges and the instrumental challenges of such optical detection.

In this work we report contact photoacoustic studies of near-field thermal and acoustic effects of radiative thermal energy transport from ablative plumes or plasmas to bulk water ablated by pulsed CO_2 laser radiation, and discuss potential implications of these effects to laser ablation applications.

[a]Author to whom correspondence should be addressed; electronic mails: skudryashov@astate.edu and sergeikudryashov@yahoo.com

II. EXPERIMENTAL SETUP

A 10.6 μm, transversely excited atmospheric (TEA) CO_2 laser beam (Lumonics 100-2, TEM_{00}, 0.1 J/pulse, with a gain-switched initial spike of duration $\tau_1 \approx 70$ ns [full width at half maximum (FWHM)] storing about $\gamma_1 \approx 50\%$ of the pulse energy, and nitrogen-fed pulse tail with a characteristic decay time of 0.6 μs, 1 Hz repetition rate) was focused by a ZnSe spherical lens (focal distance $L=10$ cm, Gaussian focal spot radius $\sigma_{1/e} \approx 0.2$ mm) at normal incidence onto a free surface of bulk de-ionized water in a plastic tube container (height $H \approx 8$ mm, diameter $D \approx 14$ mm) without bottom (Fig. 1). Laser energy was varied using a number of clear polyethylene sheets (20% attenuation per piece) and was measured in each pulse by splitting off a part of the beam to a pyroelectric detector with digital readout (Gentec ED-500). Photoacoustic studies were performed using a fast acoustic transducer ($LiNbO_3$ piezoelement, flat response in the 1–100 MHz frequency range, manufactured in the Laboratory of Laser Optoacoustics at Moscow State University), working as a bottom of the water tube container fixed by means of vacuum grease. A Lecroy storage oscilloscope (Wavepro 940) was used to record voltage transients from the transducer with no transient characteristic of laser ablation detected without the laser pulse heating the water surface. Photoacoustic measurements were performed in the fluence range $F=0.8–11$ J/cm^2, including the threshold

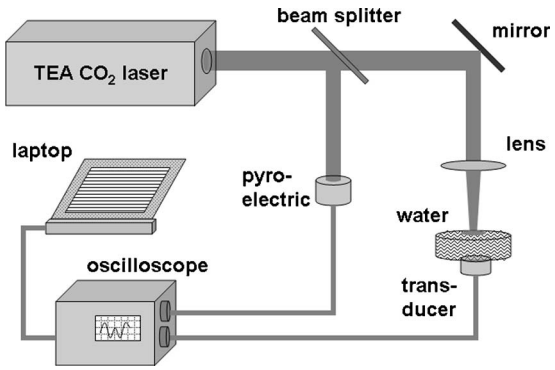

FIG. 1. Experimental setup for photoacoustic studies.

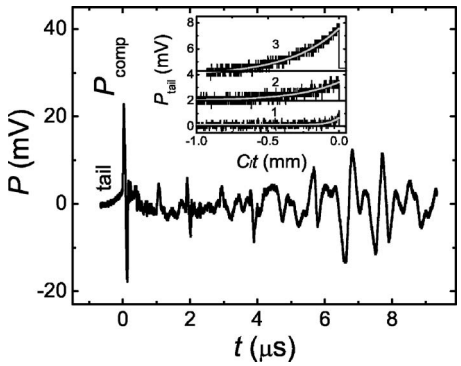

FIG. 2. Characteristic transient of acoustic pressure in water at laser fluence $F \approx 11$ J/cm^2. Inset: Characteristic acoustic tails at $F \approx 3$ (1), 8 (2), and 11 (3) J/cm^2 offset for clarity and their exponential fits.

$F_{B,S} \approx 1.7$ J/cm^2 for near-spinodal explosive boiling of water after the laser spike accompanied by expulsion of a water jet,[8] and the optical breakdown threshold in the water plume at $F_{\mathrm{pl}} \approx 7$ J/cm^2.

III. RESULTS AND DISCUSSION

A typical transient of acoustic pressure $P(t)$ under explosive boiling conditions in water at fluence $F \approx 11$ J/cm^2 $> F_{B,S}$ is shown in Fig. 2. For times $t=0-0.2$ μs this transient exhibits a main bipolar pulse described elsewhere[8] with its FWHM parameter equal to that of the main spike of the TEA laser pulse. This pulse is generated in a nonlinear thermoacoustic generation regime via the "thermal nonlinearity" mechanism,[9] corresponding to near-critical conditions for superheated water. The actual wave form with a predominant compression phase P_{comp} (positive phase in Fig. 2) characteristic of explosive boiling[10] transforms to a bipolar one due to the diffraction effect in the acoustic far field[9] where data acquisition was performed. Surprisingly, for $F > F_{B,S}$ the main acoustic pulse is preceded at negative t by a long tail whose amplitude and duration increase with increasing F (Fig. 2, inset). This tail corresponds to an acoustic signal arriving at the detector before the main pulse and could result from (1) transient variation of the penetration depth for the incident 10.6 μm CO_2 laser radiation, which is, however, usually limited to 9–11 μm;[11] (2) other acoustic, e.g., shock waves propagating faster than the ultrasonic main pulse, which should also exhibit higher amplitudes and sharp fronts rather than the rapidly diverging tail; (3) thermoacoustic generation at a free water surface corrugated due to various instabilities of surface vaporization; and (4) by the shorter-

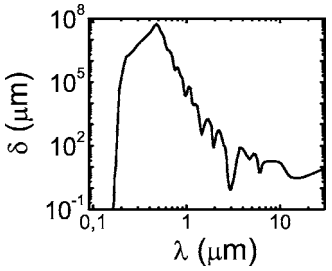

FIG. 3. Spectral dependence of penetration depth in water for electromagnetic radiation (after Ref. 11).

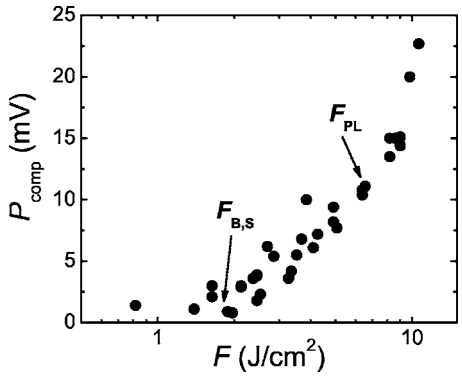

FIG. 4. Compression pulse amplitude P_{comp} vs F (marks $F_{B,S}$ and F_{pl} show the thresholds of explosive boiling of water and optical breakdown in water plume).

wavelength thermal emission of the superheated liquid and plume (or surface plasma) penetrating deeper to the water than the 10.6 μm laser radiation (Fig. 3). The latter assumption is the most consistent with the CO_2 laser heating of the vapor/droplet water plume and onset of optical breakdown acoustic generation in water plume at $F \geq F_{\mathrm{pl}} \approx 7$ J/cm^2 (Fig. 4) coinciding with the appearance of a visible spark near the water surface.

To evaluate penetration depths of thermal radiation at various incident F, the corresponding acoustic tails plotted as $P(C_l t)$ (Fig. 2, inset) for the longitudinal speed of sound in water $C_l \approx 1.4$ km/s (Ref. 12) were fitted for $t \leq 0$ using a single exponential function, $P(C_l t) = P_{\mathrm{tail}} \exp(C_l t/\delta^*)$, with an initial maximum thermoacoustic pressure amplitude P_{tail} and effective penetration depth δ^* (Fig. 5) and neglecting diffraction of plume (plasma) radiation at submillimeter distances within the liquid. The magnitude of the resulting δ^* increases from the water penetration depth, $\delta(10.6\ \mu\mathrm{m}) \approx 10$ μm,[11] at $F \geq F_{B,S}$ to a saturation level $\delta^* \approx 2 \times 10^2$ μm in the fluence range of 4–7 J/cm^2, and increasing again up to $\approx (3-3.5) \times 10^2$ μm for $F \geq 7$ J/cm^2 (Fig. 5), with the latter rise correlating with the onset of optical breakdown in water plumes for $F \geq F_{\mathrm{pl}}$ (Fig. 4). This trend of δ^* may correspond to an increase in the water plume (plasma) temperature T, which provides, according to Wien's law, a maximum spectral exitance M_λ at a characteristic wavelength $\lambda_{\max} \approx 3 \times 10^3$ μm K/T.[13] For $F_{B,S} \leq F \leq 3.7$ J/cm^2, penetration of thermal radiation is limited to approximately

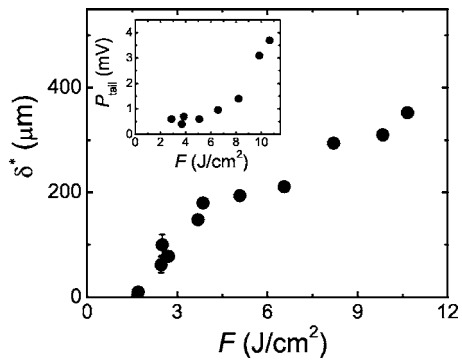

FIG. 5. Effective penetration depth δ^* and tail amplitude P_{tail} (inset) in water as a function of F.

100 μm, corresponding to maximum thermal emission at $\lambda_{max} \geqslant 2.5$ μm [see inset of Fig. 3 for the $\delta(\lambda)$ dependence of water] for $T \leqslant 1.1 \times 10^3$ K. This temperature is in agreement with estimates of water surface temperature $T_{calc}(F) \approx 293\ \mathrm{K} + \varepsilon(F)/C_p \leqslant 1.2 \times 10^3$ K for $F \leqslant 3.7$ J/cm^2, where the laser deposited volume energy density $\varepsilon(F) \approx [1 - R(10.6\ \mu\mathrm{m})]F/\delta(10.6\ \mu\mathrm{m})$ for the water reflectivity $R(10.6\ \mu\mathrm{m}) \leqslant 0.01$ (Ref. 11) and the isobaric heat capacity of water $C_p \approx 4.2$ J/K cm^3.[12] At $F \geqslant 3.7$ J/cm^2 ($T_{calc} \geqslant 1.1 \times 10^3$ K) the corresponding λ_{max} magnitudes fall in the 0.5–2.5 μm "transparency window" of water where δ^* increases to 10^3–10^7 μm (Fig. 3) and the acoustic tail signals are not strong enough to be measured with the present photoacoustic technique. Such short-wavelength thermal radiation of plumes as well as thermal and characteristic radiation resulting from collapsing steam bubbles[8,14] may photoionize water molecules or small clusters and, thus, seed optical breakdown in the water plume. The breakdown process is further driven by impact ionization of water molecules by hot electrons accelerated in the strong electric field of the intensity spikes of the CO_2 laser pulse.[1] Ionization increases the water plume (plasma) temperatures to values well above $\sim 10^4$ K.[1] An estimate of the breakdown threshold intensity for water, $I_{break} \sim 10^7$–10^8 W/cm^2 using the common expression for I_{break},[2] is consistent with the experimental threshold $F_{pl} \approx 7$ J/cm^2 ($I_{pl} \approx F_{pl}\gamma_1/\tau_1 \approx 5 \times 10^7$ W/cm^2) for breakdown occurring during the laser spike.

The $P_{tail}(F)$ curve in the inset of Fig. 5 gives insight into understanding the anomalously high amplitudes of the acoustic tails which are nearly 10% of those of corresponding main signals representing in Fig. 2 explosive boiling of water under *direct* CO_2 laser irradiation at $I_{las} \sim 10^7$ W/cm^2. At high $F \geqslant F_{pl}$ the water plume/plasma temperature T may approach values of $\sim 10^4$ K, yielding the total thermal radiation intensity (the spectral exitance M_λ integrated over the entire emission spectrum[13]) $I_{th} \sim 10^5$ W/cm$^2 \sim 10^{-2} I_{pl}$ at a characteristic $\lambda_{max} \sim 0.1$ μm, which is strongly absorbed in water (Fig. 3). There is also an enhancement factor, $\delta^*/\delta(10.6\ \mu\mathrm{m})$, for P_{tail} as compared to P_{comp} that results from different acoustic generation regimes for the tails and main signals, which are the "stress confinement" regime[15] (when $\delta^*/C_l\tau_1 \geqslant 1$) and "thermal confinement" regime[15] [when $\delta(10.6\ \mu\mathrm{m})/C_l\tau_1 \geqslant 1$], respectively. Increasing P_{tail} by a factor $\delta^*/\delta(10.6\ \mu\mathrm{m}) \sim 10^1$, one finds the thermoacoustic pressure amplitude $P_{tail} \sim I_{th}[\delta^*/\delta(10.6\ \mu\mathrm{m})] \sim 0.1 P_{comp}$ for $I_{th} \sim 10^{-2} I_{pl}$ in agreement with our experimental observations. In contrast, for 3 J/cm$^2 \leqslant F \leqslant F_{pl}$ [1.1×10^3 K $\leqslant T_{calc}(F) \leqslant 1.8 \times 10^3$ K] the corresponding peak wavelength is in the range of 1.7 μm $\leqslant \lambda_{max} \leqslant 2.5$ μm and $\delta(\lambda)$ rapidly increases from 10^2 to 10^3 μm (Fig. 3)], resulting in a much slower increase of energy deposition and water temperature versus F in the subsurface layer δ^*. As a result, P_{tail} magnitude does not change significantly in the range of 3 J/cm$^2 \leqslant F \leqslant F_{pl}$, but its absolute value remains high due to the "stress confinement" regime of acoustic generation. Above F_{pl} the amplitude increases rapidly because of the increase of absorption by the bulk water of the short-range—UV and shorter—plasma radiation despite the increasing δ^*.

Therefore, even though the near-field heating effect of thermal radiation from moderately laser-heated ablative plumes (plasmas) or surfaces ($T \sim 10^3$–10^4 K) can be neglected in the total energy balance, the related near-field thermoacoustic or thermomechanical effects may have a strong impact on steam laser cleaning of delicate nano- and microstructures using thin layers of absorbing energy transfer liquids, the precision of laser ablation of soft matter (tissues, polymers, and foams) in surgical and material science applications, and, in general, on the effective size of the heat-affected zone in laser nano- and micromodifications of solid and soft matter surfaces due to very efficient thermoacoustic generation in the stress confinement regime.

IV. CONCLUSIONS

In these contact photoacoustic studies we have experimentally studied near-field thermal and acoustic effects in bulk water induced by radiative energy transport from ablative water plumes and plasmas produced by a 10.6 μm TEA CO_2 laser. We have demonstrated that the acoustic and mechanical effects of thermal radiation can be significant in weakly absorbing soft matter materials due to acoustic (stress) generation in the "stress confinement" regime because of deep (hundreds of microns) penetration of thermal radiation emitted by high-temperature plumes.

ACKNOWLEDGMENTS

The authors are grateful to National Science Foundation and Professor Alexander A. Karabutov for financial (Grant No.0218024) and technical support, respectively.

[1] J. F. Ready, *Effects of High-Power Laser Radiation* (Academic, New York, 1971).
[2] D. Bäuerle, *Laser Processing and Chemistry* (Springer, Berlin, 2000).
[3] M. A. Shannon, X. Mao, A. Fernandez, W. T. Chan, and R. E. Russo, Anal. Chem. **67**, 2444 (1995); J. R. Ho, C. P. Grigoropoulos, and J. A. C. Humprey, J. Appl. Phys. **79**, 7205 (1996); X. Mao and R. E. Russo, Appl. Phys. A: Mater. Sci. Process. **64**, 1 (1997).
[4] S. I. Kudryashov, A. V. Pakhomov, and S. D. Allen, Proc. SPIE **5713**, 508 (2005) and references therein.
[5] S. Paul, K. Lyon, S. I. Kudryashov, and S. D. Allen, Proc. SPIE **6107**, 610709 (2006).
[6] For bibliography see, e.g., J. C. Miller and R. F. Haglund, *Laser Ablation and Desorption* (Academic, San Diego, 1998), Vol. 30, or H.-G. Rubahn, *Laser Applications in Surface Science and Technology* (Wiley, New York, 1999).
[7] I. Apitz and A. Vogel, Proc. SPIE **4961**, 48 (2003); M. H. Niemz, *Laser-Tissue Interactions* (Springer, Berlin, 2004).
[8] S. I. Kudryashov, K. Lyon, and S. D. Allen, Phys. Rev. E **73**, 055301 (2006); Appl. Phys. Lett. **88**, 214105 (2006); Proc. SPIE **6086**, 60861Y (2006).
[9] V. E. Gusev and A. A. Karabutov, *Laser Optoacoustics* (AIP, New York, 1993).
[10] F. V. Bunkin, A. A. Kolomensky, V. G. Mikhailevich, S. M. Nikiforov, and A. M. Rodin, Sov. Phys. Acoust. **32**, 21 (1986); R. O. Esenaliev, A. A. Karabutov, N. B. Podymova, and V. S. Letokhov, Appl. Phys. B: Lasers Opt. **59**, 73 (1994); D. Kim and C. P. Grigoropoulos, Appl. Surf. Sci. **127–129**, 53 (1998).

[11]R. K. Shori, A. A. Walston, O. M. Stafsudd, D. Fried, and J. T. Walsh, Jr., IEEE J. Sel. Top. Quantum Electron. **7**, 959 (2001); E. D. Palik, *Handbook of Optical Constants of Solids* (Academic, San Diego, 1985).
[12]I. S. Grigor'ev and E. Z. Meilikhov, *Fizicheskie Velichini* (Energoatomizdat, Moscow, 1991).
[13]R. McCluney, *Introduction to Radiometry and Photometry* (Artech House, Boston, 1994).
[14]S. I. Kudryashov, K. Lyon, and S. D. Allen, Phys. Rev. E (submitted).
[15]E. Leveugle, D. S. Ivanov, and L. V. Zhigilei, Appl. Phys. A: Mater. Sci. Process. **79**, 1643 (2004).